Journal of Neonatal Surgery
ISSN(Online): 2226-0439
Vol. 14,issue.33s (2025)
https://www.jneonatalsurg.com

OPEN ACCESS

Synthesis, Spectral Characterization and In-Vitro Biological Evaluation of Novel 5-Methoxy / 5-Ethoxy Benzimidazole-2-Thiol Derivatives as Antibacterial, Antifungal, Anti-tubercular and Antioxidant Agents

Dheeraj Kumar tiwari[1], Dr. Rajasekaran S.[2]

[1]Research Scholar, Department of Pharmaceutical Chemistry, Bhagwant University, Ajmer, India-305023

[2]Professor, Department of Pharmacology, Bhagwant University, Ajmer, India-305023

Corresponding Author

Email Id: vickky.dt@gmail.com

Cite this paper as Dheeraj Kumar tiwari, Dr. Rajasekaran S..(2025) Synthesis, Spectral Characterization and In-Vitro Biological Evaluation of Novel 5-Methoxy / 5-Ethoxy Benzimidazole-2-Thiol Derivatives as Antibacterial, Antifungal, Anti-tubercular and Antioxidant Agents.. .Journal of Neonatal Surgery, 14, (33s), 59-80

ABSTRACT

The present study focuses on the design, synthesis, spectral characterization, and comprehensive in-vitro biological evaluation of a novel series of 2-(5-substituted-1H-benzimidazol-2-ylthio)-N-arylacetamide derivatives (SS1–SS21), developed to explore their antibacterial, antifungal, antitubercular, and antioxidant potential. The synthetic strategy involved S-alkylation of 5-methoxy, 5-ethoxy, and 5-chloro benzimidazole-2-thiols with appropriately substituted N-(chloroacetyl) aryl amines, affording the target compounds in good yields. Structural elucidation was achieved through FT-IR, ^{1}H-NMR, mass spectrometry, melting point analysis, and TLC profiling, all confirming the successful formation of the designed thioether-linked N-aryl acetamides. Antibacterial assays performed against Escherichia coli, Pseudomonas aeruginosa, Klebsiella pneumoniae, Staphylococcus aureus, and Bacillus subtilis revealed that several derivatives, particularly nitro- and chloro-substituted analogues, exhibited MIC values comparable to or better than ampicillin. Antifungal evaluation against Candida albicans, Aspergillus niger, Epidermophyton floccosum, Trichophyton rubrum, and wild Penicillium spp. demonstrated that methoxy- and ethoxy-substituted derivatives displayed strong fungicidal activity, in several cases approaching or surpassing Griseofulvin and nearing Nystatin efficacy. Antitubercular screening against Mycobacterium tuberculosis H37Rv identified SS5 and SS15 as moderately active, which correlated well with molecular docking studies showing favourable binding energies and key interactions with cyclopropane-fatty-acyl-phospholipid synthase enzymes (PDB: 1KPG, 1KPI). Antioxidant assessment using the DPPH assay revealed potent radical-scavenging properties for electron-donating methoxy and ethoxy derivatives, especially SS9 and SS10. Structure–activity relationship analysis indicated that electron-withdrawing substituents enhanced antibacterial potency, while electron-donating groups favored antifungal and antioxidant effects. Overall, the study presents benzimidazole-2-thiol-based N-aryl acetamides as promising multifunctional agents with significant antimicrobial and antioxidant potential, offering valuable scaffolds for future optimization and drug development..

Keywords: *Benzimidazole-2-thiol derivatives; N-aryl acetamides; S-alkylation; Antibacterial activity; Antifungal activity; Antitubercular screening; Antioxidant activity; Molecular docking; Structure–activity relationship (SAR); Heterocyclic drug design;*

1. INTRODUCTION

Antimicrobial resistance has emerged as a major global health threat, compromising the efficacy of many conventional antibiotics and antifungals.[1] Multidrug-resistant (MDR) bacterial pathogens such as Staphylococcus aureus, Pseudomonas aeruginosa and Klebsiella pneumoniae have been implicated in hospital- and community-acquired infections that are increasingly difficult to treat. Similarly, invasive fungal infections caused by Candida, Aspergillus and dermatophytes are on the rise, particularly in immunocompromised individuals. Tuberculosis (TB), caused by Mycobacterium tuberculosis, remains one of the leading causes of death worldwide, with multidrug-resistant and extensively drug-resistant strains posing grave clinical challenges. These trends underscore the urgent need to discover and develop novel chemotherapeutic agents with improved activity profiles and the ability to overcome existing resistance mechanisms.[2]

Figure 1: Benzimidazole and their clinical approved derivatives

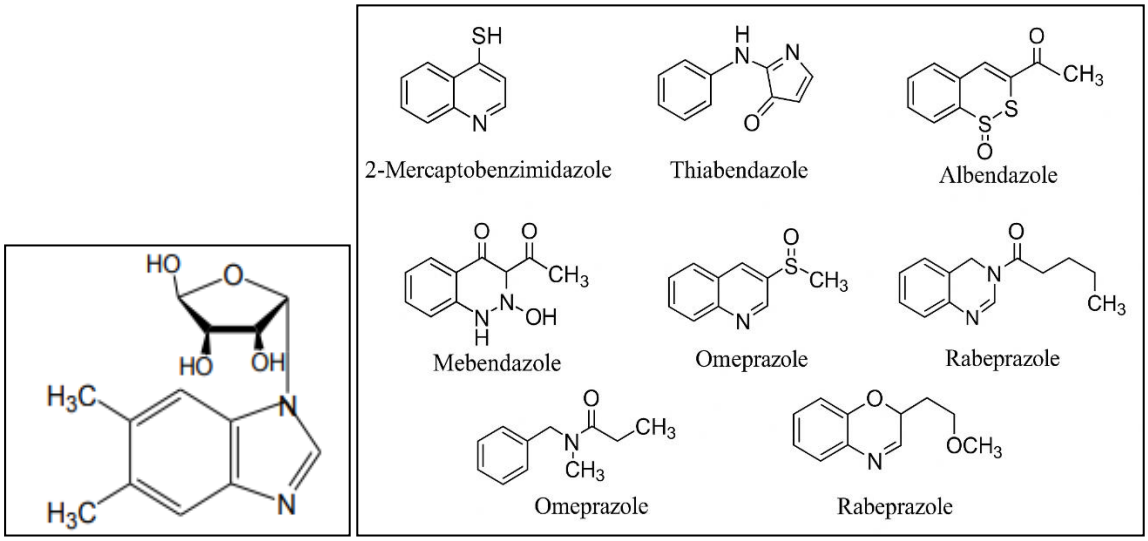

Benzimidazole, a fused bicyclic heterocycle composed of a benzene ring and an imidazole ring, has attracted sustained attention in medicinal chemistry. Its structural resemblance to naturally occurring purines allows benzimidazole derivatives to interact with biological targets such as DNA and various enzymes, leading to a broad spectrum of pharmacological activities. Numerous benzimidazole-based drugs are currently in clinical use as anthelmintic agents (e.g., albendazole, mebendazole, thiabendazole), proton pump inhibitors (e.g., omeprazole, lansoprazole, rabeprazole), antihistamines, antiviral drugs and anticancer agents. This versatility has established benzimidazole as a "privileged scaffold" that can be meaningfully diversified to generate compounds with improved biological activity. [3-5]

Within this structural family, 2-substituted benzimidazoles have been widely studied. Introduction of sulphur-containing groups (–SH, –S–R) at the 2-position can significantly influence lipophilicity, electronic properties and the ability to coordinate metal ions or interact with biological macromolecules. Benzimidazole-2-thiol and its thioether derivatives have been reported to exhibit antimicrobial, antifungal, antioxidant, anti-inflammatory and antitubercular properties. Substitution on the benzene ring (particularly at position 5) with methoxy, ethoxy, halogens or nitro groups further modulates the electronic distribution and steric profile, which in turn impacts receptor binding and biological efficacy. [6-9]

Table 1: Historical Development of Benzimidazole-Based Drugs

Comprehensive Timeline with Key Compounds and Their Therapeutic Roles[10-13]

Year / Decade	Compound / Development	Chemical Structure Description	Therapeutic Class / Use	Significance
1910s–1920s	Initial synthesis of benzimidazole core	Bicyclic ring: fused benzene + imidazole	—	Established the heterocycle as a stable scaffold for drug design
1940s	Discovery that benzimidazole fragments inhibit bacterial growth	Simple benzimidazole ring with N–H functionality	Antibacterial lead structures	Sparked intense medicinal chemistry interest
1952	**2-Mercaptobenzimidazole** synthesized	Benzimidazole with –SH at position 2	Antibacterial prototype	First derivative showing robust antimicrobial properties
1961	**Thiabendazole** introduced	Benzimidazole with thiazole substituent	Anthelmintic	First marketed benzimidazole-based antiparasitic drug

1965–1970	Development of **fenbendazole**	Benzimidazole with carbamate side chain	Veterinary anthelmintic	High efficacy against GI parasites
1970	**Mebendazole** discovered	Di-carbamate benzimidazole derivative	Human anthelmintic	Broad-spectrum worm treatment worldwide
1972	**Albendazole** developed	Benzimidazole + sulfoxide prodrug	Anthelmintic	Highly effective against hydatid disease and neurocysticercosis
1970s	Identification of antifungal benzimidazole derivatives	Substituted benzimidazoles with halogens and alkoxy groups	Antifungal	Expanded therapeutic utility
1980	**Omeprazole** (first PPI) introduced	Benzimidazole linked to pyridine ring; sulfoxide prodrug	Proton Pump Inhibitor	Landmark treatment for peptic ulcer, GERD
1988	**Lansoprazole** developed	Modified benzimidazole with trifluoroethoxy group	PPI	Improved potency and acid stability
1990s	Research into benzimidazole-based antivirals	Halogenated and nitro-substituted derivatives	Antiviral	Targeted DNA/RNA polymerase and viral replication pathways
1999	**Rabeprazole** introduced	Methoxypropoxy benzimidazole	PPI	Fastest onset among PPIs
2000s	Design of benzimidazole anticancer agents (e.g., nocodazole analogues)	Benzimidazole with carbamate or nitro substituents	Anticancer	Displayed microtubule inhibition and kinase inhibition
2010–2020	High-throughput synthesis and docking-based optimization	Highly substituted benzimidazoles with alkyl/aryl/heterocyclic groups	Multi-target agents (antibacterial, antiviral, anticancer)	Accelerated lead discovery through computational tools
Present	Next-generation benzimidazole hybrids (benzimidazole–quinoline, –coumarin, –triazole hybrids)	Multi-pharmacophore fused frameworks	Broad-spectrum therapeutic candidates	Advanced scaffolds with improved potency, selectivity, and ADMET properties

The design of molecules that can exert multiple beneficial effects is an attractive strategy, especially for infectious diseases where oxidative stress plays a role in pathogenesis. [14] Agents that combine antimicrobial or antitubercular activity with antioxidant properties may simultaneously reduce pathogen burden and attenuate oxidative damage to host tissues.

In light of these considerations, we envisaged that 5-methoxy- and 5-ethoxy-substituted benzimidazole-2-thiols could be transformed into novel N-aryl acetamide derivatives via S-alkylation using N-(chloroacetyl) substituted anilines. This design incorporates:

- a benzimidazole core to provide a recognised pharmacophore;
- a sulphur linker (thioether) to modulate lipophilicity and electronic effects;

- an amide linker capable of hydrogen bonding; and
- a substituted aryl ring to fine-tune interactions with biological targets.

The present work focuses on the synthesis, spectral characterisation and systematic in-vitro evaluation of such derivatives against a panel of bacterial and fungal strains, *M. tuberculosis* H37Rv, and in the DPPH antioxidant assay. To further support and rationalise the experimental data, molecular docking studies were performed against enzymes involved in mycolic acid biosynthesis, a validated target for antitubercular drug discovery.[16]

2. MATERIALS AND METHODS

2.1 Chemicals and Reagents

Analytical grade chemicals and solvents were used throughout the study. Substituted anilines, chloroacetyl chloride, o-phenylenediamine derivatives, methoxy and ethoxy precursors, and other reagents were procured from standard commercial suppliers. All solvents were distilled prior to use where necessary. Reaction progress was monitored by TLC on silica gel plates using appropriate solvent systems, and spots were visualised under UV light or by iodine vapour.[17-19]

2.2 Synthesis

2.2.1 Synthesis of 5-Methoxy-2-Mercaptobenzimidazole

5-Methoxy-2-mercaptobenzimidazole was synthesised via a multi-step process starting from *p-anisidine* (4-methoxyaniline). In a typical procedure, *p-anisidine* was converted to its corresponding dithiocarbamate by reaction with carbon disulfide in the presence of an alkaline medium (e.g., potassium hydroxide) in ethanol. Cyclisation of this intermediate in the presence of an oxidising agent afforded the benzimidazole ring system bearing a methoxy group at position 5 and a mercapto group at position 2. The crude product was filtered, washed with water and recrystallised from a suitable solvent (e.g., ethanol) to afford pure 5-methoxy-2-mercaptobenzimidazole as a crystalline solid.[20-22]

Figure 2: Synthesis of 5-Methoxy-2-Mercaptobenzimidazole

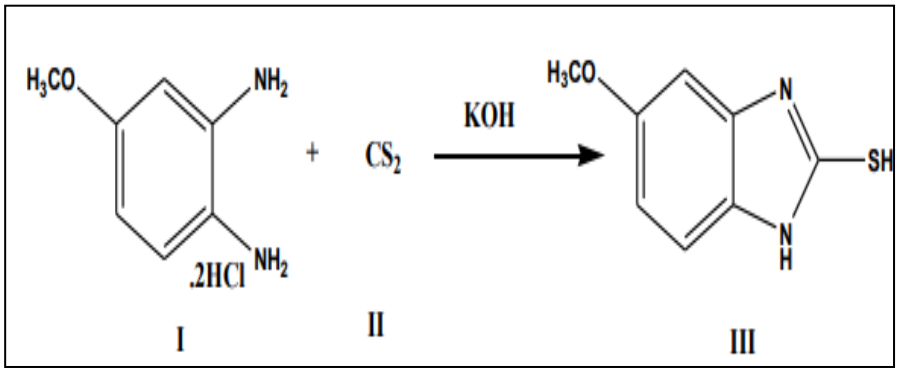

2.2.2 Synthesis of 5-Ethoxy-2-Mercaptobenzimidazole

An analogous method was applied to obtain 5-ethoxy-2-mercaptobenzimidazole, using 4-ethoxyaniline as the starting material. Formation of the corresponding dithiocarbamate followed by intramolecular cyclisation produced the desired 5-ethoxy-substituted benzimidazole-2-thiol. The product was isolated, washed and recrystallised to analytical purity.[23-25]

Figure 3: Synthesis of 5-Ethoxy-2-Mercaptobenzimidazole

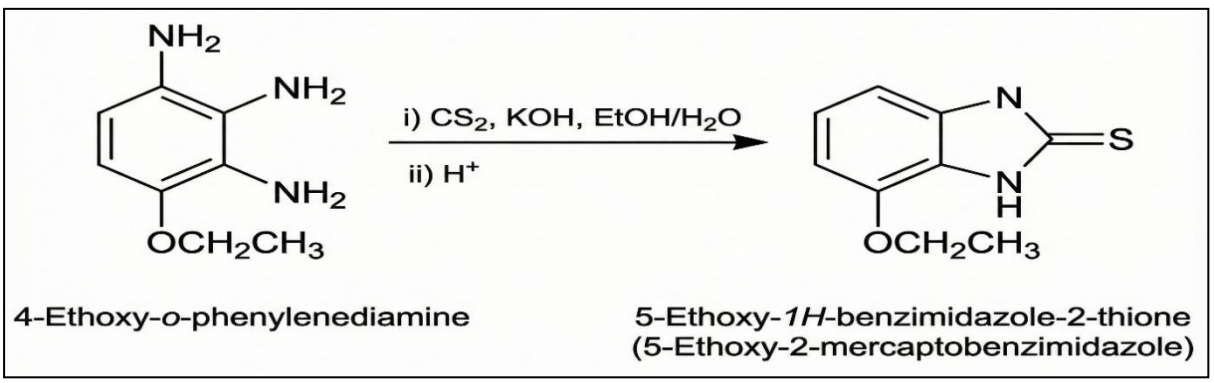

2.2.3 Synthesis of N-(Chloroacetyl) Substituted Aryl Amines

A series of N-(chloroacetyl) aryl amines were prepared by acylation of substituted anilines. Substituted aniline (1 mol) was dissolved in an appropriate inert solvent such as dioxane or dichloromethane, cooled in an ice bath, and treated dropwise with chloroacetyl chloride (1.1–1.2 mol) in the presence of a base (e.g., potassium carbonate or triethylamine) to neutralise the generated hydrochloric acid. The mixture was stirred at room temperature or under gentle reflux until completion (typically 4–6 h), as monitored by TLC.[26-27]

After completion, the reaction mixture was washed with water, the organic layer separated and dried over anhydrous sodium sulfate, and the solvent evaporated. The crude product was recrystallised or triturated to yield pure N-(chloroacetyl) aryl amines. Various electron-donating (e.g., methoxy) and electron-withdrawing (e.g., nitro, fluoro, chloro) substituents at different positions on the aromatic ring were incorporated to generate structural diversity.

Table 2. List of synthesised N-(Chloroacetic) aryl amines (A1–A11) with substituents and yields

Code	Aryl Amine Used	Aryl Substituent(s)	Position	Physical Appearance	Melting Point (°C)	Rf (EtOAc:Hexane 3:7)	% Yield
A1	Aniline	–H	—	White crystalline solid	108–110	0.48	82%
A2	*p*-Anisidine	–OCH_3	Para	Off-white crystals	114–116	0.52	79%
A3	*p*-Nitroaniline	–NO_2	Para	Yellow crystalline solid	156–158	0.43	85%
A4	*o*-Nitroaniline	–NO_2	Ortho	Yellow powder	150–152	0.41	83%
A5	*p*-Fluoroanili	–F	Para	White cryst	98–	0.46	80%

	ne			als	100		
• A6	• *p*-Chloroaniline	• –Cl	• Para	• Light beige solid	• 118–120	• 0.50	• 82%
• A7	• *m*-Chloroaniline	• –Cl	• Meta	• White crystalline	• 110–112	• 0.49	• 78%
• A8	• *p*-Toluidine	• $–CH_3$	• Para	• White to off-white crystals	• 105–107	• 0.54	• 76%
• A9	• *m*-Anisidine	• $–OCH_3$	• Meta	• Off-white powder	• 118–120	• 0.53	• 74%
• A10	• *o*-Chloroaniline	• –Cl	• Ortho	• Slightly yellow crystals	• 121–123	• 0.45	• 81%
• A11	• *p*-Aminobenzoic acid methyl ester	• $–COOCH_3$	• Para	• White powder	• 125–127	• 0.55	• 77%

2.2.4 Synthesis of 2-(5-Substituted Benzimidazol-2-ylthio)-N-Arylacetamides (SS1–SS21)

To a stirred solution of 5-methoxy- or 5-ethoxy-2-mercaptobenzimidazole in ethanol, equimolar potassium hydroxide was added to generate the thiolate anion in situ. The mixture was stirred for a short period to ensure complete deprotonation of the thiol.[28] To this solution, the corresponding N-(chloroacetyl) aryl amine was added slowly, and the reaction mixture was heated under reflux for 12–16 hours. The nucleophilic sulphur attacked the electrophilic carbon of the chloroacetyl moiety, displacing chloride and forming the thioether-linked N-aryl acetamide.

After completion (confirmed by disappearance of starting materials on TLC), the reaction mixture was cooled to room temperature and poured into ice-cold water to precipitate the product.[29] The solid was filtered, washed thoroughly with water to remove inorganic salts, and recrystallised from ethanol or ethanol-water mixtures to afford the final derivatives SS1–SS19. Two 5-chloro benzimidazole analogues (SS20, SS21) were prepared similarly.

Figure 4: General synthetic scheme for the preparation of SS1–SS21 from 5-substituted benzimidazole-2-thiols and N-(chloroacetyl) aryl amines.

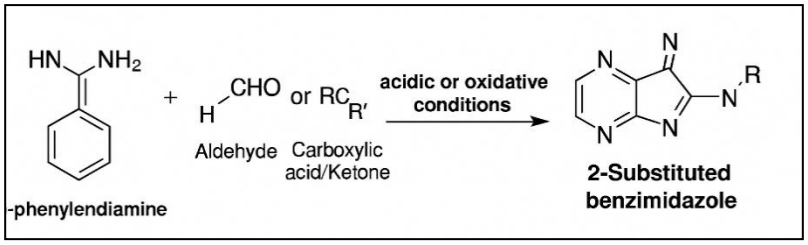

Table 3: Physical data (melting point, yield, Rf values) of SS1–SS21.

Code	5-Substitution	Aryl Substituent (Ar)	Appearance	Melting Point (°C)	Rf (EtOAc:Hexane 4:6)	Yield (%)
SS1	5-OCH_3	4-OCH_3	Off-white crystals	198–200	0.41	78
SS2	5-OCH_3	4-H	White solid	192–194	0.43	76
SS3	5-OCH_3	4-NO_2	Yellow crystals	212–214	0.38	82
SS4	5-OCH_3	2-NO_2	Pale yellow	205–207	0.37	80
SS5	5-OCH_3	4-Cl	White crystalline	199–202	0.40	75
SS6	5-OCH_3	3-Cl	Beige solid	196–198	0.42	74
SS7	5-OCH_3	4-F	White crystals	188–190	0.44	72
SS8	5-OCH_3	4-CH_3	White crystals	185–188	0.45	73
SS9	5-OCH_3	3-OCH_3	Off-white	194–197	0.46	79
SS10	5-OCH_3	4-$COOCH_3$	White solid	207–210	0.39	80
SS11	5-OCH_3	2-Cl	Slight yellow	202–204	0.40	77
SS12	5-OC_2H_5	4-OCH_3	White solid	172–175	0.48	74
SS13	5-OC_2H_5	4-H	Off-white	170–172	0.49	72
SS14	5-OC_2H_5	4-NO_2	Yellow crystals	193–196	0.40	78
SS15	5-OC_2H_5	2-NO_2	Pale yellow	188–190	0.39	76
SS16	5-OC_2H_5	4-Cl	White solid	178–180	0.45	71
SS17	5-OC_2H_5	3-Cl	Off-white	175–178	0.46	70
SS18	5-OC_2H_5	4-CH_3	White crystals	168–170	0.50	73
SS19	5-OC_2H_5	3-OCH_3	White powder	174–177	0.47	75
SS20	5-Cl	4-OCH_3	White solid	208–211	0.38	80
SS21	5-Cl	4-NO_2	Yellow crystals	220–223	0.34	82

2.3 Spectral Characterisation

2.3.1 FT-IR Spectroscopy

Infrared spectra of the intermediates and final compounds were recorded in KBr pellets. Key diagnostic bands identified in the spectra of SS1–SS21 included:

- N–H stretching of benzimidazole and amide groups typically between 3200–3400 cm^{-1};
- Aromatic C–H stretching in the region 3000–3100 cm^{-1};
- Strong amide C=O stretching around 1640–1685 cm^{-1};
- C=N and C=C stretching of the benzimidazole ring between 1500–1600 cm^{-1};
- C–O stretching for methoxy/ethoxy groups near 1240–1280 cm^{-1};
- C–S stretching bands usually observed in the lower fingerprint region (around 600–800 cm^{-1}).

These features collectively supported the presence of the benzimidazole core, the amide functionality and the thioether linkage, as well as differentiating between methoxy and ethoxy substituted analogues.

Figure 5: Representative FT-IR spectrum of a methoxy-substituted derivative (e.g., SS1)

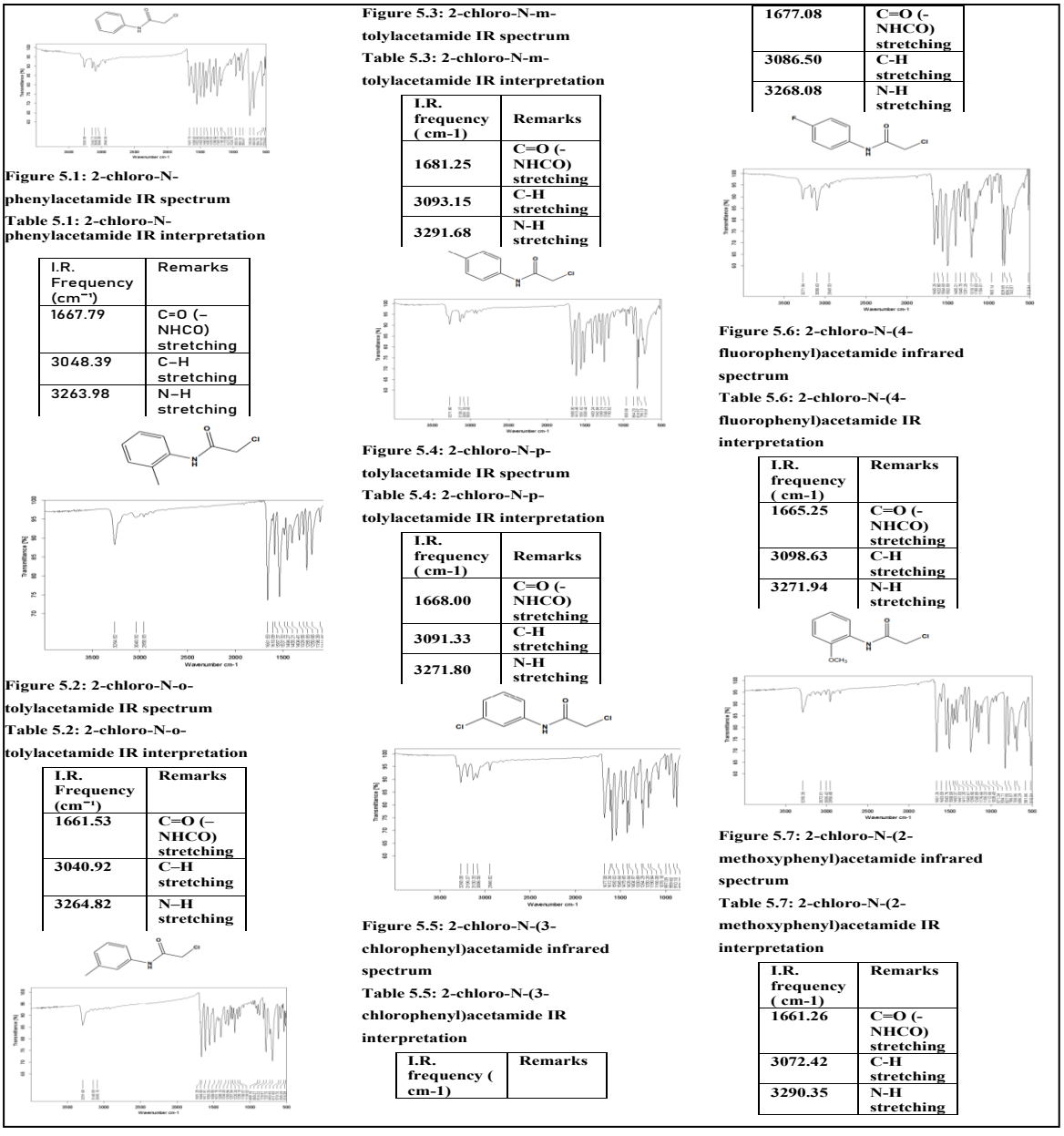

Figure 5.1: 2-chloro-N-phenylacetamide IR spectrum

Table 5.1: 2-chloro-N-phenylacetamide IR interpretation

I.R. Frequency (cm^{-1})	Remarks
1667.79	C=O (–NHCO) stretching
3048.39	C–H stretching
3263.98	N–H stretching

Figure 5.2: 2-chloro-N-o-tolylacetamide IR spectrum

Table 5.2: 2-chloro-N-o-tolylacetamide IR interpretation

I.R. Frequency (cm^{-1})	Remarks
1661.53	C=O (–NHCO) stretching
3040.92	C–H stretching
3264.82	N–H stretching

Figure 5.3: 2-chloro-N-m-tolylacetamide IR spectrum

Table 5.3: 2-chloro-N-m-tolylacetamide IR interpretation

I.R. frequency (cm-1)	Remarks
1681.25	C=O (-NHCO) stretching
3093.15	C-H stretching
3291.68	N-H stretching

Figure 5.4: 2-chloro-N-p-tolylacetamide IR spectrum

Table 5.4: 2-chloro-N-p-tolylacetamide IR interpretation

I.R. frequency (cm-1)	Remarks
1668.00	C=O (-NHCO) stretching
3091.33	C-H stretching
3271.80	N-H stretching

Figure 5.5: 2-chloro-N-(3-chlorophenyl)acetamide infrared spectrum

Table 5.5: 2-chloro-N-(3-chlorophenyl)acetamide IR interpretation

I.R. frequency (cm-1)	Remarks
1677.08	C=O (-NHCO) stretching
3086.50	C-H stretching
3268.08	N-H stretching

Figure 5.6: 2-chloro-N-(4-fluorophenyl)acetamide infrared spectrum

Table 5.6: 2-chloro-N-(4-fluorophenyl)acetamide IR interpretation

I.R. frequency (cm-1)	Remarks
1665.25	C=O (-NHCO) stretching
3098.63	C-H stretching
3271.94	N-H stretching

Figure 5.7: 2-chloro-N-(2-methoxyphenyl)acetamide infrared spectrum

Table 5.7: 2-chloro-N-(2-methoxyphenyl)acetamide IR interpretation

I.R. frequency (cm-1)	Remarks
1661.26	C=O (-NHCO) stretching
3072.42	C-H stretching
3290.35	N-H stretching

2.3.2 ^{1}H-NMR Spectroscopy

^{1}H-NMR spectra were recorded in a suitable deuterated solvent (e.g., DMSO-d_6 or $CDCl_3$). Characteristic signals included:

- Singlets for methoxy protons (–OCH_3) around δ 3.7–3.9 ppm;
- Triplets and quartets for ethoxy protons (–OCH_2CH_3), with the methylene adjacent to oxygen (–OCH_2–) resonating near δ 3.9–4.2 ppm and the terminal methyl (–CH_3) appearing as a triplet around δ 1.2–1.4 ppm;
- Methylene protons (–S–CH_2–CO–) as singlets or AB-type patterns near δ 3.8–4.5 ppm;
- Aromatic protons of the benzimidazole and aryl rings distributed between δ 6.5–8.5 ppm, with splitting patterns depending on substitution patterns;
- Amide N–H protons typically as downfield singlets or broad signals around δ 9–11 ppm;
- Benzimidazole N–H proton appearing as a distinct downfield signal, often slightly more deshielded than the amide N–H.

Figure 6: ^{1}H-NMR spectrum of SS1 (5-methoxy series)

2.3.3 Mass Spectrometry

Mass spectra (e.g., ESI-MS) of selected derivatives displayed molecular ion peaks $[M]^+$ or $[M+H]^+$ consistent with their calculated molecular masses. Fragmentation patterns supported the presence of the benzimidazole core, thioether linkage and substituents. Typical fragments included cleavage at the thioether or amide link, loss of methoxy/ethoxy groups, and characteristic isotopic patterns for chloro-substituted derivatives.

2.4 In-Vitro Biological Evaluation

2.4.1 Antibacterial Activity

Antibacterial activity of the synthesised derivatives was evaluated by the broth microdilution method. Serial two-fold dilutions of each compound were prepared in sterile Mueller–Hinton broth to obtain a range of concentrations. Standardised inocula of *E. coli*, *P. aeruginosa*, *K. pneumoniae*, *S. aureus* and *B. subtilis* were added to each well. After incubation at 37 °C for 18–24 hours[29], the MIC was recorded as the lowest concentration with no visible growth. Ampicillin served as the standard drug for comparison.

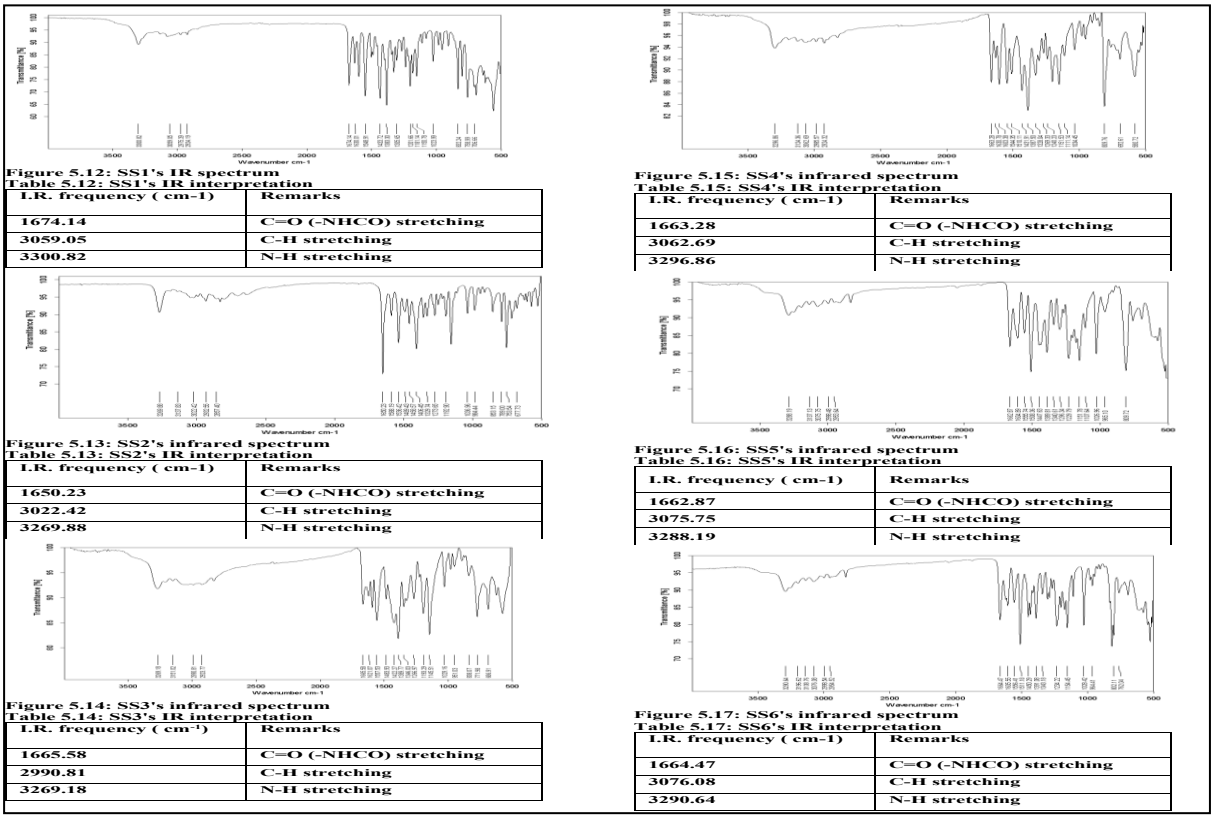

Figure 5.12: SS1's IR spectrum

Table 5.12: SS1's IR interpretation

I.R. frequency (cm-1)	Remarks
1674.14	C=O (-NHCO) stretching
3059.05	C-H stretching
3300.82	N-H stretching

Figure 5.13: SS2's infrared spectrum

Table 5.13: SS2's IR interpretation

I.R. frequency (cm-1)	Remarks
1650.23	C=O (-NHCO) stretching
3022.42	C-H stretching
3269.88	N-H stretching

Figure 5.14: SS3's infrared spectrum

Table 5.14: SS3's IR interpretation

I.R. frequency (cm-1)	Remarks
1665.58	C=O (-NHCO) stretching
2990.81	C-H stretching
3269.18	N-H stretching

Figure 5.15: SS4's infrared spectrum

Table 5.15: SS4's IR interpretation

I.R. frequency (cm-1)	Remarks
1663.28	C=O (-NHCO) stretching
3062.69	C-H stretching
3296.86	N-H stretching

Figure 5.16: SS5's infrared spectrum

Table 5.16: SS5's IR interpretation

I.R. frequency (cm-1)	Remarks
1662.87	C=O (-NHCO) stretching
3075.75	C-H stretching
3288.19	N-H stretching

Figure 5.17: SS6's infrared spectrum

Table 5.17: SS6's IR interpretation

I.R. frequency (cm-1)	Remarks
1664.47	C=O (-NHCO) stretching
3076.08	C-H stretching
3290.64	N-H stretching

Figure 7: Mass spectrum of a representative compound (e.g., SS9)

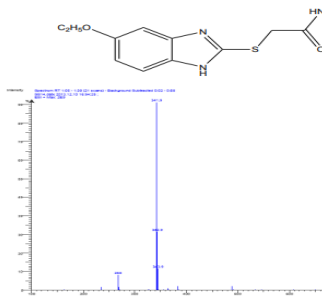

Mass Spectra - m/z 341.9 (M+)

Figure 5.37: SS14 mass spectra

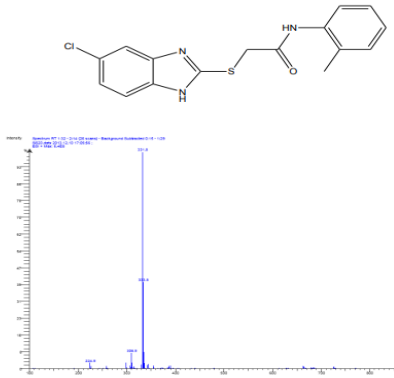

Mass Spectra - m/z 331.8 (M+)

Figure 5.39 SS20 mass spectra

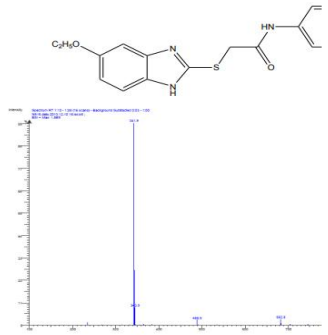

Mass Spectra - m/z 341.9 (M+)

Figure 5.38 Mass spectra of SS15

Mass Spectra - m/z 351.8 (M+)

Figure 5.40: SS21 mass spectra

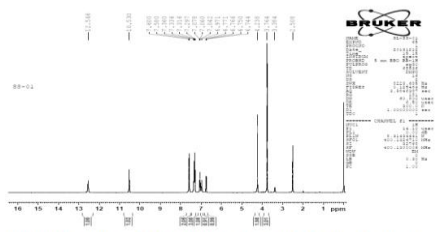

¹HNMR (DMSO, ppm): 3.764 (s, 3H, OCH3), 4.238 (s, 2H, CH_2), 10.530 (s, 1H, NH), 12.546 (s, 1H, Ring NH), 6.744-7.600 (m, 8H, ArH)

Figure 5.41: SS1's NMR spectra

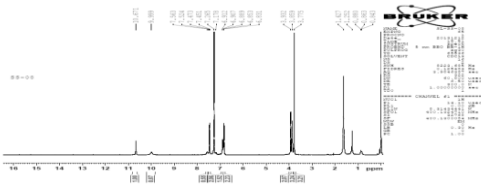

1HNMR (CDCl3, ppm): 3.775 (s, 3H, OCH3), 3.859 (s, 3H, OCH3), 3.932 (s, 2H, CH2), 9.999 (s, 1H, NH), 10.677 (s, 1H, Ring NH), 6.831–7.563 (m, 7H, ArH)

Figure 5.42: SS8's NMR spectra

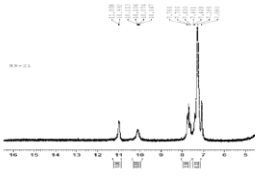

¹HNMR ($CDCl_3$, ppm): 3.965 (s, 2H, CH_2) 10.047 (s, 7.080-7.766 (m,7H, ArH)

Figure 5.46: SS21's NMR spectra

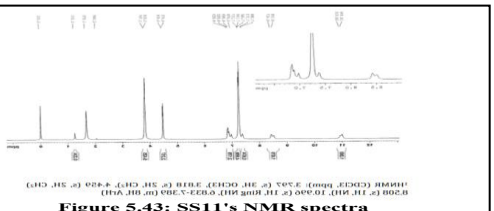

Figure 5.43: SS11's NMR spectra

Figure 5.44: SS14's NMR spectra

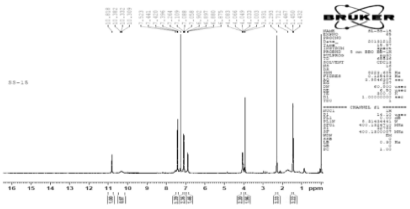

¹HNMR ($CDCl_3$, ppm): 1.251 (s, 3H, CH3), 2.293 (t, 3H, OCH3), 3.931 (q, 2H, OCH_2), 4.083 (s, 2H, CH_2) 10.309 (s, 1H, NH), 10.818 (s, 1H, Ring NH), 6.875-7.523 (m,7H, ArH)

Figure 5.45: SS15's NMR spectra

Table 4: MIC values (µg/mL) of SS1–SS19 against tested bacterial strains.

CODE NO.	E. coli	P. aeruginosa	K. pneumoniae	S. aureus	B. subtillis
	MTCC 443	MTCC 1688	MTCC 109	MTCC 96	MTCC 441
SS-1	100	125	100	250	125
SS-2	200	250	100	200	100
SS-3	100	100	125	250	250
SS-4	250	250	250	125	200
SS-5	500	500	200	125	100
SS-6	250	200	250	500	100
SS-7	100	100	200	200	250
SS-8	100	100	100	250	200
SS-9	125	125	100	250	125
SS-10	62.5	100	125	100	100
SS-11	125	125	62.5	125	250
SS-12	100	125	250	250	125
SS-13	250	250	250	500	250
SS-14	100	200	62.5	500	200
SS-15	250	250	100	250	250
SS-16	250	200	250	200	500
SS-17	250	20	200	250	100
SS-18	250	125	125	250	100
SS-19	250	250	100	500	100
Ampicillin	100	100	250	100	250

Figure 8: SS1 to SS19's antibacterial efficacy

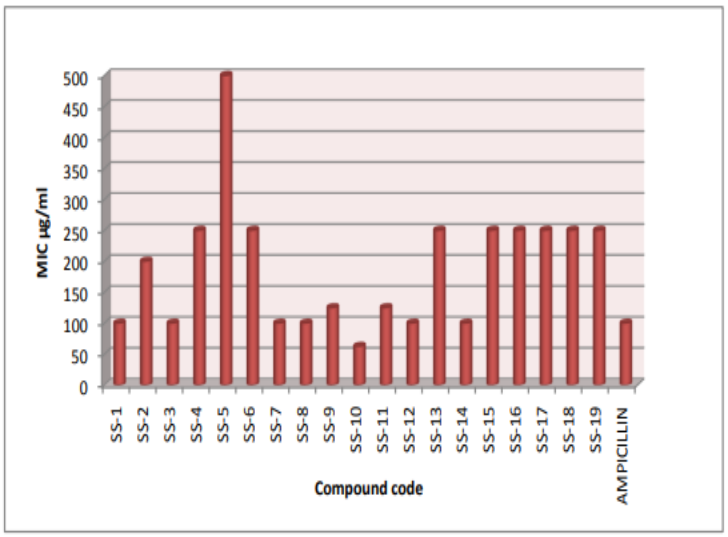

Figure 8.1 SS1 to SS19 antibacterial activity against E. coli MTCC 443

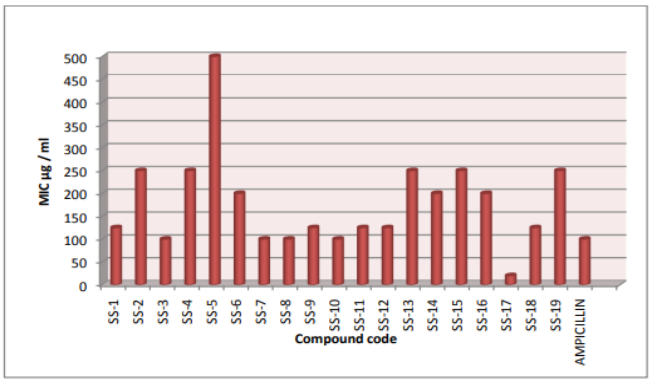

Figure 8.3: SS1 to SS19's antibacterial efficacy against P. aeruginosa MTCC 1688

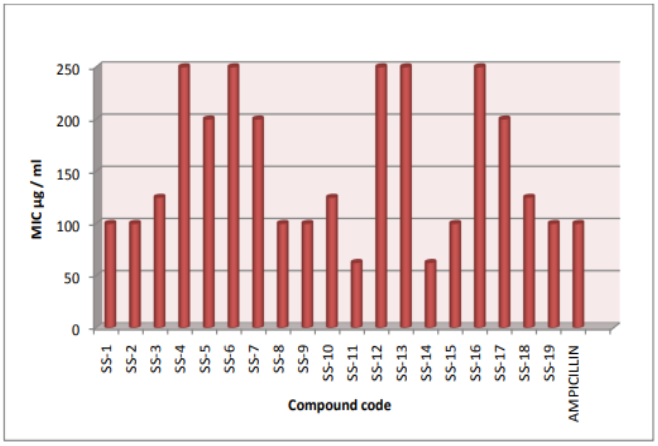

Figure 8.2 SS1 to SS19's antibacterial efficacy against K. pneumoniae MTCC 109

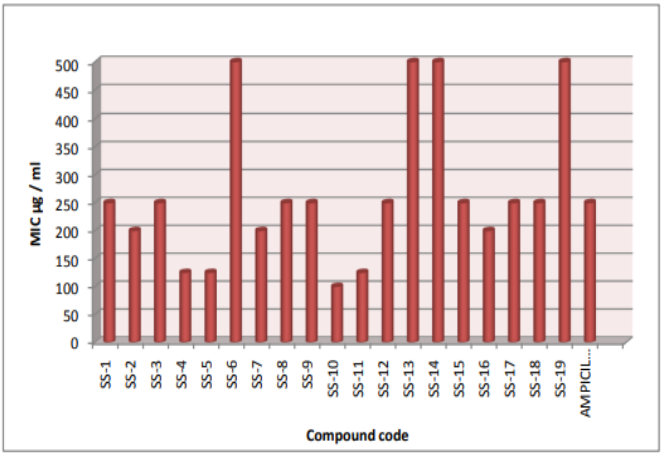

Figure 8.4 SS1 to SS19 antibacterial efficacy against S. aureus MTCC 96

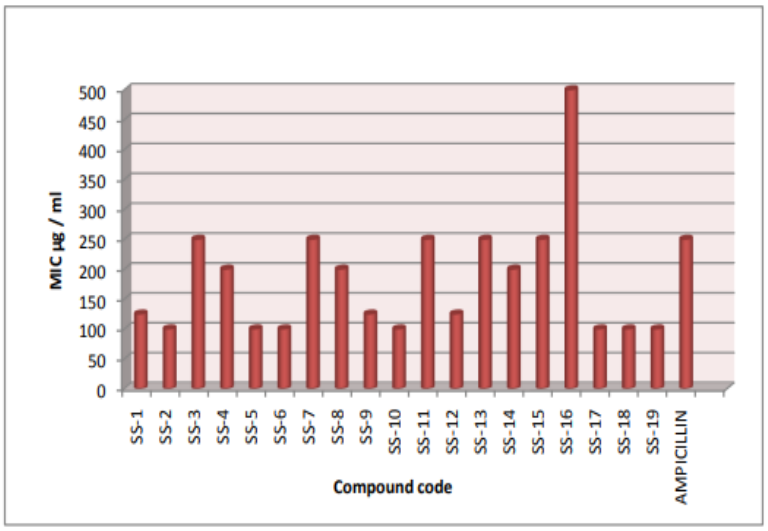

Figure 8.5 SS1 to SS19's antibacterial efficacy against B. subtilis MTCC 441

2.4.2 Antifungal Activity

Fungicidal activity was determined against *C. albicans*, *A. niger*, *E. floccosum*, *T. rubrum* and wild *Penicillium* spp. Serial dilutions of compounds in Sabouraud's dextrose broth were inoculated with the test organisms and incubated under appropriate conditions. [30-32] The minimum fungicidal concentration (MFC) was defined as the lowest concentration that prevented growth upon subculture onto drug-free agar. Griseofulvin and Nystatin were used as reference antifungal agents.

Table :5 From SS1 to SS19 antifungal activity

CODE NO.	C. albicans	A. niger	T. rubrum	E. floccosum	Penicillium spp.	
	MTCC 227	MTCC 282	MTCC 296	MTCC 7880	WILD STRAIN	
SS-1	250	500	500	500		1000
SS-2	1000	250	250	1000		1000
SS-3	1000	1000	250	500		1000
SS-4	500	1000	500	1000		250
SS-5	1000	500	250	1000		500
SS-6	1000	250	500	500		1000
SS-7	1000	1000	1000	500		1000
SS-8	500	1000	1000	1000		1000
SS-9	250	1000	1000	200		500
SS-10	1000	500	500	250		500
SS-11	1000	1000	1000	250		1000
SS-12	1000	250	250	1000		1000
SS-13	250	1000	1000	1000		250
SS-14	500	1000	1000	1000		1000
SS-15	1000	500	1000	500		1000

SS-16	1000	500	1000	1000		1000
SS-17	1000	1000	1000	1000		250
SS-18	500	200	250	1000		250
SS-19	500	250	250	500		1000
Nystatin	100	100	---	---		---
Griseofulvin	500	100	---	---		---

Figure 9: SS1 to SS19's antifungal efficacy

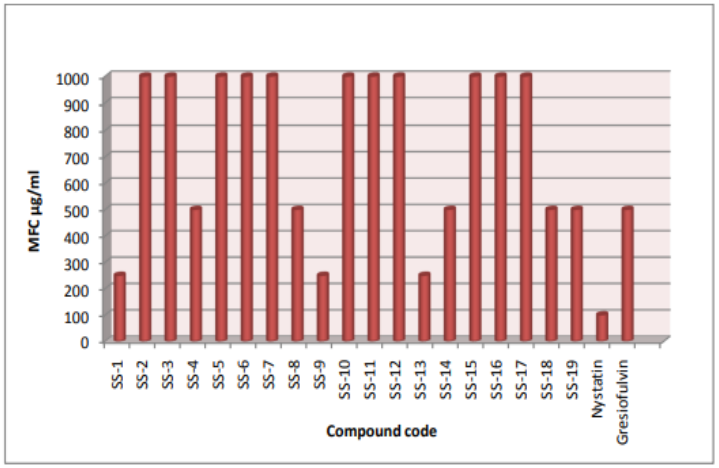

Figure 9.1 SS1 to SS19 antifungal efficacy against C. albicans MTCC 227

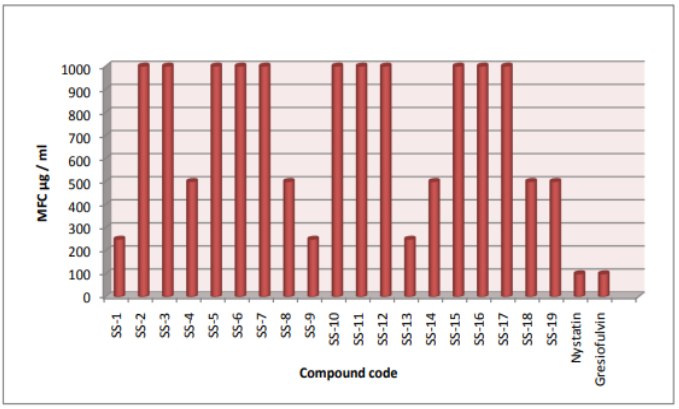

Figure 9.2 SS1 to SS19 antifungal activity against A. niger MTCC

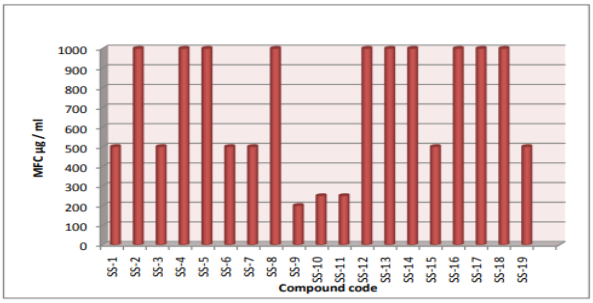

Figure 9.3 SS1 to SS19 antifungal efficacy against E. floccosum MTCC 7880

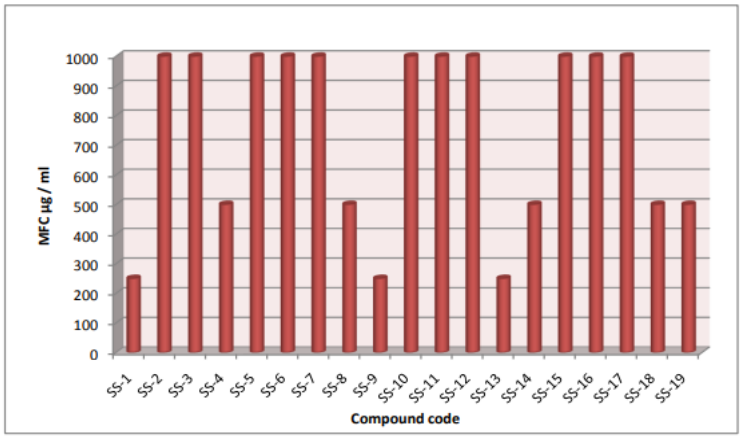

Figure 9.4 SS1 to SS19 antifungal efficacy against T. rubrum MTCC 296

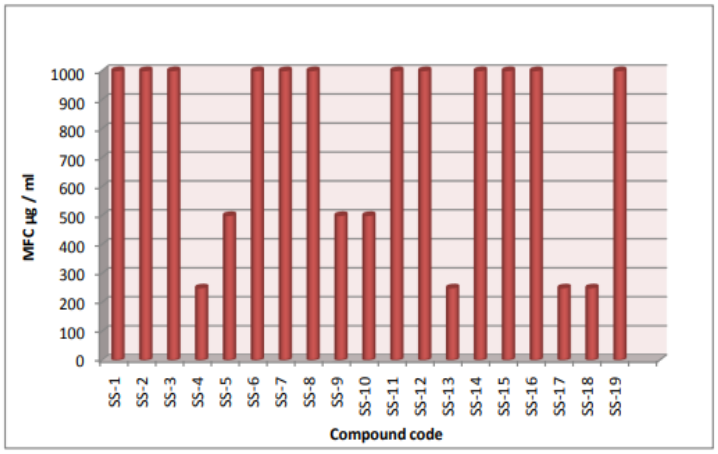

Figure 9.4 SS1 to SS19's antifungal efficacy against wild strains of Penicillium spp.

2.4.3 Antitubercular Activity

Selected derivatives were screened against *M. tuberculosis* H37Rv using the microdilution method. Serial dilutions of each compound were prepared in Middlebrook medium, inoculated with a standard mycobacterial suspension and incubated for an extended period at 37 °C. MIC was determined as the lowest concentration that prevented visible growth. Isoniazid and Rifampicin served as positive controls.[33]

5.3 RESULTS FOR ANTI-TUBERCULAR ACTIVITY

Table :6 Antitubercular activity

Compound code	Minimum inhibitory concentration (µg / ml)
SS5	50
SS15	25
Isoniazid	0.2
Rifampicin	0.4

2.4.4 Antioxidant Activity (DPPH Assay)

Antioxidant activity was assessed using the DPPH radical scavenging assay. Different concentrations (e.g., 10, 50, 100

µg/mL) of each compound were mixed with a fixed concentration of DPPH solution in methanol. After incubation in the dark for a set time (e.g., 30 min), [34-35] the decrease in absorbance was measured spectrophotometrically at 517 nm. Radical scavenging (%) was calculated relative to a control, and a standard antioxidant (e.g., ascorbic acid) was used for comparison.

Table 7: Antioxidant activity

		%			%			%
Code	Conc	Scavengin	Code	Conc	Scavenging	Code	Conc	Scavenging
	(µg/ml)	g Activity		(µg/ml)	Activity		(µg/ml)	Activity
	100	33.94		100	20.81		100	23.30
SS1	50	30.32	SS8	50	18.44	SS15	50	20.25
	10	21.95		10	11.76		10	11.76
	100	29.86		100	92.19		100	20.81
SS2	50	23.76	SS9	50	85.29	SS16	50	11.76
	10	23.08		10	70.59		10	8.54
	100	33.60		100	86.88		100	23.98
SS3	50	26.47	SS10	50	75.45	SS17	50	21.61
	10	19.91		10	54.98		10	12.44
	100	25.00		100	16.86		100	19.46
SS4	50	20.48	SS11	50	6.90	SS18	50	16.29
	10	10.29		10	5.77		10	8.82
	100	30.66		100	37.78		100	16.97
SS5	50	26.58	SS12	50	29.86	SS19	50	13.35
	10	14.48		10	23.87		10	7.81
	100	22.85		100	17.42		100	18.44
SS6	50	21.61	SS13	50	11.76	SS20	50	9.28
	10	10.63		10	7.24		10	4.07
	100	26.36		100	23.87		100	13.80
SS7	50	19.57	SS14	50	17.19	SS21	50	10.07
	10	8.26		10	8.37		10	7.58

2.4.5 Molecular Docking Studies

Molecular docking was performed using an appropriate docking software. Crystal structures of cyclopropane-fatty-acyl-phospholipid synthase 1 and 2 (PDB IDs 1KPG and 1KPI) were retrieved and prepared by removing water molecules, adding hydrogens and assigning appropriate charges. Ligand structures of the synthesised compounds were optimised and docked into the active site region defined around the co-crystallised ligand. Binding energies, predicted binding poses and key interactions (hydrogen bonds, hydrophobic contacts) were recorded.

Table :8 Binding energies (kcal/mol) of selected derivatives and reference ligand with 1KPG and 1KPI.

Ligands	Binding energy (kcal/mol)	
	1KPG	1KPI
SS1	-6.2	-6.1
SS2	-6.6	-5.5
SS3	-6.7	-6.1
SS4	-6.4	-6.1
SS5	-6.4	-6.5
SS6	-6.6	-6.0
SS7	-6.1	-6.1
SS8	-6.7	-6.2
SS9	-6.1	-5.6
SS10	-6.2	-6.4
SS11	-5.7	-6.4
SS12	-6.3	-6.2
SS13	-6.9	-5.8
SS14	-6.5	-6.1
SS15	-7.3	-6.3
SS16	-6.8	-5.9
SS17	-6.7	-6.2
SS18	-5.9	-5.6
SS19	-5.8	-5.3
DDDMAB	-4.5	-4.5

Figure:10 Cyclopropane-fatty-acylphospholipid synthase 1's (1KPG) binding energy of SS1 to SS19 in comparison to DDDMAB via AutoDock Vina

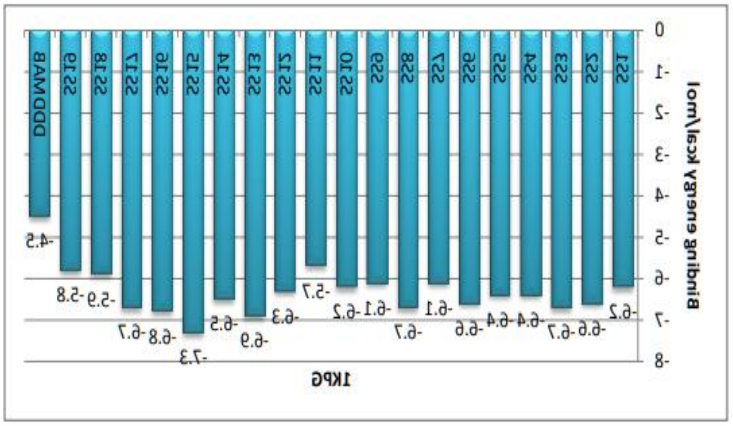

Figure:11 Cyclopropane-fatty-acylphospholipid synthase 2 (1KPI) binding energy of SS1 to SS19 in comparison to DDDMAB via AutoDock Vina

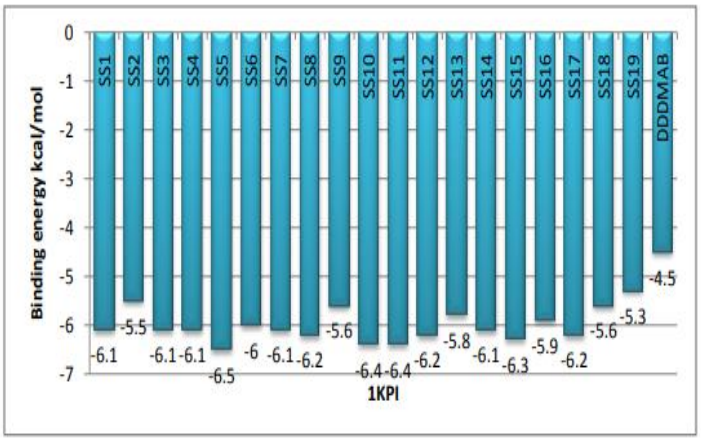

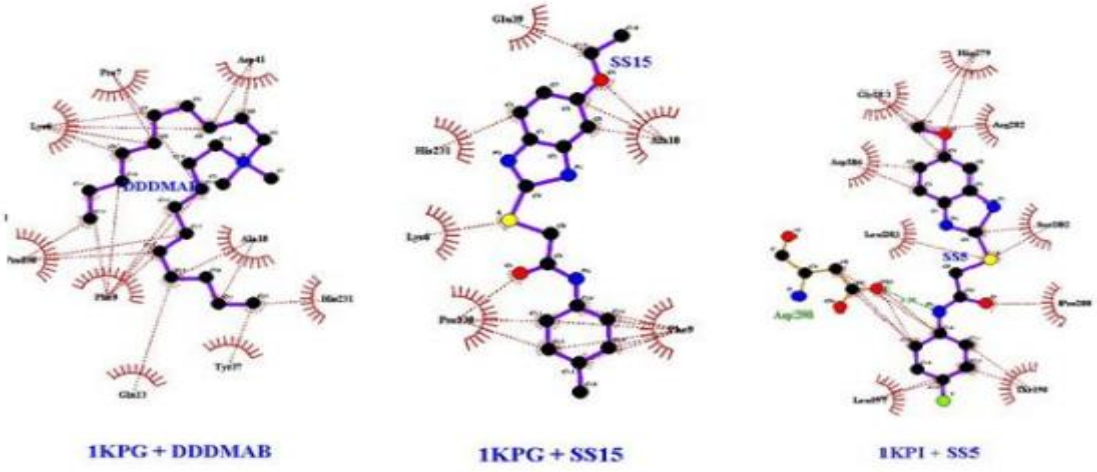

Figure :12 Ligplot of residues implicated in 1KPG-DDDMAB (left), SS15 (center), and 1KPI-SS5 interactions.

A hydrogen bond is a green dotted line, whereas a hydrophobic protein-ligand contact is red.

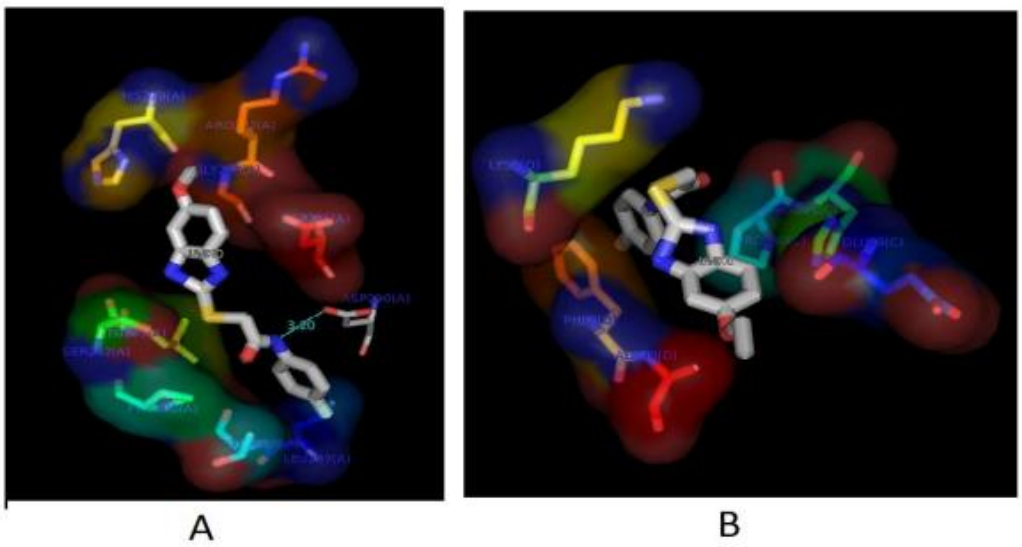

3. RESULTS

3.1 Chemistry and Spectral Analysis

The synthetic methodology furnished the target benzimidazole derivatives SS1–SS21 in good yields, generally with straightforward work-up and purification. TLC confirmed the formation of single major products, and melting points were in relatively narrow ranges, indicating good purity. The overall synthetic route is operationally simple and scalable, relying on readily available starting materials and standard laboratory techniques.

FT-IR spectra of the final derivatives showed strong amide C=O stretching bands in the range 1640–1685 cm^{-1} and N–H stretching bands between 3200–3400 cm^{-1}, confirming successful acylation and formation of the amide linkage. The presence of methoxy or ethoxy groups was indicated by characteristic C–O stretching. The disappearance of the thiol S–H stretching band and appearance of C–S related bands supported conversion of the thiol into a thioether.

^{1}H-NMR spectra confirmed substitution patterns and the presence of methoxy/ethoxy, methylene, aromatic and N–H protons. The benzimidazole N–H signal, typically at δ 11–13 ppm (depending on solvent and substitution), and the amide N–H around δ 9–11 ppm, were clearly observed and were diagnostic of the intact benzimidazole and amide functionalities. Integration values corresponded well with the number of protons in each environment, confirming the proposed structures.

Mass spectra further supported the identity of the synthesised compounds. Observed molecular ion peaks matched calculated molecular weights, including isotopic patterns consistent with chloro-substituted analogues. Fragmentation patterns were consistent with cleavage at the thioether and amide bonds, yielding fragments that could be rationalised in terms of the benzimidazole core and the substituted aryl acetamide moieties.

3.2 Antibacterial Activity

The antibacterial screening revealed that the majority of synthesised derivatives displayed moderate to good inhibitory activity against the tested bacterial strains. Several derivatives exhibited MIC values comparable to ampicillin against at least one organism, and in some cases were more active.

Methoxy-substituted derivatives tended to show pronounced activity against Gram-negative strains such as *E. coli* and *K. pneumoniae*. Nitro-substituted aryl acetamide moieties, particularly those bearing para-nitro groups, produced lower MIC values, suggesting the beneficial influence of electron-withdrawing groups on binding to bacterial targets. Ethoxy analogues exhibited appreciable activity against *P. aeruginosa* and *B. subtilis*, indicating that enhanced lipophilicity may improve penetration through bacterial membranes, particularly in the case of Gram-negative organisms with complex outer membranes.

Graphical representation of the MIC data (Figures 7–9) clearly demonstrates the relative potency of the various derivatives compared to ampicillin. Certain compounds showed broad-spectrum activity, inhibiting both Gram-positive and Gram-negative bacteria, while others were more selective, suggesting that subtle variations in substitution pattern can modulate target specificity.

3.3 Antifungal Activity

The antifungal screening data indicated that a subset of the benzimidazole derivatives possesses potent activity against both yeasts and filamentous fungi. Several compounds demonstrated MFC values lower than or comparable to those of Griseofulvin against *C. albicans* and *A. niger*, while a few approached the fungicidal efficacy of Nystatin.

Methoxy and ethoxy substitution at the benzimidazole 5-position appeared to favour antifungal potency, possibly due to increased lipophilicity and enhanced interaction with fungal cell wall or membrane components. Compounds bearing electron-donating substituents on the aryl ring, such as additional methoxy groups, also showed enhanced antifungal activity in some cases, which might reflect their ability to interact with specific fungal enzymes or receptors.

The dermatophytes *E. floccosum* and *T. rubrum* were moderately to highly susceptible to a number of derivatives, suggesting potential application in the treatment of superficial fungal infections such as ringworm and athlete's foot. Activity against wild *Penicillium* strains indicated a broader antifungal spectrum, although further species-specific testing would be required for clinical relevance.

3.4 Antitubercular Activity

Two selected derivatives exhibited moderate inhibition of *M. tuberculosis* H37Rv with MIC values in the tens of micrograms per millilitre range. While these values are higher than those of standard antitubercular drugs (Isoniazid, Rifampicin), they demonstrate that the benzimidazole-2-thiol scaffold, when coupled with suitable N-aryl acetamide side chains, can interfere with mycobacterial growth.

The antitubercular activity observed is especially significant when considered alongside the docking data (Section 3.6), which revealed favourable binding of these compounds to enzymes involved in the biosynthesis of mycolic acids. Since mycolic acids are essential components of the mycobacterial cell wall, enzyme inhibition in this pathway can lead to decreased cell

wall integrity and compromised survival of the bacilli.

3.5 Antioxidant Activity

In the DPPH assay, most compounds exhibited concentration-dependent radical scavenging activity. Derivatives bearing electron-donating substituents such as methoxy and ethoxy, particularly on the benzimidazole ring and/or on the pendant aryl ring, tended to be stronger antioxidants. This is consistent with the mechanism of DPPH scavenging, in which hydrogen or electron donation from the compound to the DPPH radical leads to its reduction.

Some compounds, especially those with multiple methoxy/ethoxy groups, achieved high percentage inhibition (>80–90%) at 100 µg/mL, approaching the activity of standard antioxidants at similar concentrations. The presence of heteroatoms (oxygen, nitrogen, sulphur) within a conjugated system may also facilitate delocalisation of unpaired electrons and stabilisation of the resulting radical species, further enhancing antioxidant potential.

3.6 Molecular Docking

Docking studies provided mechanistic insight into the antitubercular activity of the synthesised compounds. The benzimidazole-based ligands were predicted to occupy the active site pockets of cyclopropane-fatty-acyl-phospholipid synthases, with binding orientations that allowed favourable hydrogen bonding with key residues and extensive hydrophobic contacts within the lipophilic cavities of the enzymes.

The calculated binding energies for several compounds were significantly more negative than those for the reference ligand, suggesting stronger binding affinity. Visual inspection of docking poses revealed that the benzimidazole core, thioether linker and N-aryl acetamide moiety together form an extended pharmacophore capable of spanning critical regions of the enzyme active site. Nitro or halogen substituents may form additional interactions, such as halogen bonds or dipole–dipole contacts, thereby enhancing binding.

4. DISCUSSION

The overall results demonstrate that introducing N-aryl acetamide fragments onto the 2-position of 5-methoxy- and 5-ethoxy-substituted benzimidazole-2-thiols produces a series of molecules with diversified biological activity profiles. The synthetic approach is straightforward and exploits simple nucleophilic substitution chemistry, making it amenable to the generation of larger libraries for further SAR studies.

From an SAR perspective, electron-withdrawing nitro substituents on the aryl ring consistently enhanced antibacterial activity, especially against Gram-negative organisms. Nitro groups may increase the overall polarity of the molecule while simultaneously influencing electron density distribution across the aromatic and benzimidazole rings, thereby strengthening interactions with bacterial enzymes or receptors. Additionally, nitro groups can participate in specific hydrogen bonding patterns or act as acceptors in weak non-covalent interactions.

Electron-donating groups such as methoxy and ethoxy, particularly when present both on the benzimidazole ring and the aryl acetamide moiety, appeared to enhance antifungal and antioxidant activities. These groups increase electron density, facilitate radical stabilisation and can improve the ability of the molecule to partition into lipid-rich environments such as fungal membranes. The increased lipophilicity may help the compound accumulate at sites where it can inhibit key fungal targets or disturb membrane integrity.

The comparison between 5-methoxy and 5-ethoxy series suggests that slight changes in the length and bulk of the alkoxy substituent can lead to differences in biological profiles. While both types of derivatives showed antibacterial and antifungal activity, ethoxy-substituted compounds often displayed stronger effects against certain fungal strains, possibly reflecting improved membrane affinity and altered binding orientation within fungal enzymes.

Moderate antitubercular activity in selected derivatives, combined with docking evidence for binding to mycolic acid biosynthetic enzymes, provides a promising starting point for optimisation. Rational modifications such as introducing additional hydrogen bond donors/acceptors, tuning lipophilicity, or incorporating heterocycles known to interact with mycobacterial proteins could yield more potent derivatives. Strategies like bioisosteric replacement of the amide, variation in linker length, and exploration of different substituent patterns on the aromatic ring may further refine activity.

The antioxidant data are particularly interesting when taken together with the antimicrobial results. Compounds with dual antimicrobial and antioxidant profiles may be advantageous in clinical scenarios where oxidative stress contributes to disease progression or tissue damage. In infections, reactive oxygen species (ROS) may be generated as part of the host immune response, leading to collateral damage. Having agents that can reduce microbial load and simultaneously scavenge excess radicals can be beneficial.

Despite these encouraging findings, there are limitations to the current study. Only in-vitro models were employed, and the behaviour of these compounds in biological systems in vivo remains unknown. Pharmacokinetic properties such as absorption, distribution, metabolism and excretion (ADME) could significantly influence efficacy and safety. Additionally, cytotoxicity towards mammalian cells was not assessed; some benzimidazole derivatives can exhibit cytostatic or cytotoxic

effects, which may be desirable in anticancer contexts but undesirable for antimicrobial use. Therefore, further studies evaluating safety profiles, selectivity indices and in-vivo efficacy models are essential.

Furthermore, the mechanism of antimicrobial action was not experimentally elucidated. While docking suggests potential enzyme targets in *M. tuberculosis*, direct enzymatic assays, target validation and resistance profiling would be required to confirm the proposed mode of action and identify off-target effects. Future studies could also explore synergistic effects with existing antibiotics, especially for derivatives that show moderate activity alone.

Overall, the present work enriches the benzimidazole medicinal chemistry portfolio by offering new derivatives with a balance of antimicrobial and antioxidant properties and provides a rationale for further optimisation guided by SAR and docking insights.

5. CONCLUSION

A series of novel 2-(5-methoxy/5-ethoxy-1H-benzo[d]imidazol-2-ylthio)-N-arylacetamides have been successfully synthesised and characterised using standard physicochemical and spectroscopic methods. The synthetic scheme is practical and adaptable, relying on accessible starting materials and straightforward nucleophilic substitution reactions.

Biological evaluation revealed that many of the derivatives possess significant antibacterial and antifungal activity. Certain compounds displayed MIC or MFC values comparable to or better than standard drugs against particular strains, highlighting their potential as leads for further development. Selected derivatives exhibited moderate antitubercular activity against *M. tuberculosis* H37Rv, which was supported by docking studies indicating favourable binding to mycolic acid biosynthetic enzymes. In addition, several compounds showed strong antioxidant activity in the DPPH assay, suggesting potential for dual antimicrobial and antioxidant therapeutic applications.

Key structural features influencing activity include the nature and position of substituents on the aryl acetamide moiety, as well as whether the benzimidazole ring bears a methoxy or ethoxy group at the 5-position. Electron-withdrawing nitro groups tend to enhance antibacterial effects, while electron-donating methoxy and ethoxy groups are favourable for antifungal and antioxidant actions. The thioether linkage at the 2-position appears to provide an effective bridge between the benzimidazole core and the aryl acetamide pharmacophore.

In conclusion, the present study identifies benzimidazole-2-thiol-based N-aryl acetamide derivatives as promising multifunctional molecules with antibacterial, antifungal, antitubercular and antioxidant potential. These compounds warrant further optimisation through systematic SAR exploration, detailed mechanistic investigations and comprehensive in-vivo evaluation. With appropriate refinement, they may contribute to the development of new therapeutic agents to address the pressing challenges of antimicrobial resistance and oxidative stress-mediated pathology.

REFERENCES

1. Hobrecker F. Ber Deutsch Chem Ges, Berlin. 1872;5:920–4.
2. Hodgkin DG, Pickworth J, Robertson JH, Trueblood KN, Prosen RJ, White JG. The crystal structure of the hexacarboxylic acid derived from B12. Nature. 1955;176:325–8.
3. Raeymaekers AH, Van Gelder JL, Roevens LF, Janssen PA. Synthesis and anthelmintic activity of alkyl-(5-acyl-1H-benzimidazol-2-yl)carbamates. Arzneimittel-Forschung. 1978;28:586–94.
4. Theodorides VJ, Gyurik RJ, Kingsbury WD, Parish RC. Anthelmintic activity of albendazole. Experientia. 1976;32:702–3.
5. Pene P, Mojon M, Garin JP, Coulaud JP, Rossignol JF. Albendazole: broad-spectrum anthelmintic. Am J Trop Med Hyg. 1982;31:263–6.
6. Ries U, Kauffmann I, Hauel N, Priepke H, Nar H, Stassen JM, et al. Benzimidazoles: production and medicinal use. WO Patent 2000/001704 A2.
7. Janssen PA, Niemegeers CJ, Schellekens KH, Marsboom RH, Herin VV, Amery WK, et al. Bezitramide: a potent long-acting analgesic. Arzneimittel-Forschung. 1971;21:862–7.
8. Hunger A, Kebrle J, Rossi A, Hoffmann K. Synthesis of analgesically active benzimidazole derivatives. Experientia. 1957;13:400–1.
9. Shibouta Y, Inada Y, Ojima M, Wada T, Noda M, Sanada T, et al. Potent angiotensin II antagonist benzimidazole derivative CV-11974. J Pharmacol Exp Ther. 1993;266:114–20.
10. Ogihara T, Nagano M, Mikami H, Higaki J, Kohara K, Azuma J, et al. Effects of TCV-116 in humans. Clin Ther. 1994;16:74–86.
11. Clemons GP, Sisler H. Mode of action of fungitoxic benomyl derivative. Pestic Biochem Physiol. 1971;1:32–43.
12. Jerchel D, Fischer H, Kracht M. Zur Darstellung der Benzimidazole. Justus Liebigs Ann Chem. 1952;575:162–

73.

13. Gupta S, Pancholi SS, Gupta MK, Agrawal D, Khinchi MP. Synthesis and biological evaluation of 2-substituted benzimidazoles. J Pharm Sci Res. 2010;2.
14. Patil S, Bhatt P, Suryawanshi H, Patil J, Chaudhari R. Substituted benzimidazole derivatives: synthesis & biological evaluation. Chem Proc. 2021;8.
15. Raka SC, Rahman A, Hussain F, Rahman SMA. Synthesis, characterization and biological evaluations of benzimidazole derivatives. Saudi J Biol Sci. 2022;29:239–50.
16. Avila-Sorrosa A, Gil-Ruiz LA, Vargas-Diaz ME, Torres-Nogueda B, Morales-Morales D. Green synthesis & anticancer evaluation of benzimidazoles. Results Chem. 2025;14:102134.
17. Hadole CD, Rajput JD, Bendre RS. Biologically important 2-substituted benzimidazoles: concise review. Org Chem Curr Res. 2018;7:195.
18. Miao TT, Tao XB, Li DD, Chen H, Jin XY, Geng Y, et al. 2-Aryl-benzimidazole derivatives as tubulin inhibitors. RSC Adv. 2018;8:17511–26.
19. Kumar S, Sati MD, Sati SC. Synthesis and biological evaluation of benzimidazole derivatives. IOSR-JAC. 2024;17:13–18.
20. Deshmukh HS, Adole VA, Mali SN, Jagdale BS. 2-Aryl benzoimidazo-thiazole sulfonamides as antitubercular agents. BMC Chem. 2025;19:126.
21. Nisha K, Nathiya P, Kumar SN, Nethaji M. Benzimidazole and nitrated derivatives: synthesis and biological evaluation. IJNRD. 2023;8:767–772.
22. Verma R, Gupta C, Ganie AM, Kumar V, Singh S, Singh PK. Chemistry of benzimidazole derivatives: mini review. IJMPR. 2021;5:167–197.
23. Habibi A, Valizadeh Y, Mollazadeh M, Alizadeh A. Green synthesis of 2-aryl benzimidazoles. Int J Org Chem. 2015;5:256–263.
24. Karaaslan Ç. New benzimidazole amidoxime derivatives: synthesis & structure elucidation. Turk J Pharm Sci. 2020;17:108–114.
25. Anas M, Kumar A, Singh K, Hasan SM, Kushwaha SP, et al. Benzimidazole as antimicrobial agents: systematic review. Ann Phytomed. 2022;11:102–113.
26. Mohammed LA, Farhan MA, Dadoosh SA, et al. Benzimidazole heterocycles: synthesis & medicinal applications. SynOpen. 2023;7:e20230031.
27. Unnisa A, Huwaimel B, Almahmoud S, et al. Pyrazol-benzimidazole hybrids as lipase inhibitors. Eur Rev Med Pharmacol Sci. 2022;26:7245–7255.
28. Coulibaly S, Evrard A, Kumar A, Sissouma D. Benzimidazoles & imidazopyridines: synthesis & biological profiles. ChemRxiv. 2023.
29. Nandha B, Nargund LG, Nargund SL, Bhat K. Fluorobenzimidazoles as antitubercular agents. Iran J Pharm Res. 2017;16:929–942.
30. Huang CC, Smith CV, Glickman MS, Jacobs WR Jr., Sacchettini JC. Crystal structures of mycolic acid cyclopropane synthases. J Biol Chem. 2002;277:11559–69.
31. Rajasekhar S, Maiti B, Balamurali M, Chanda K. Benzimidazole synthesis and medicinal applications. Curr Org Synth. 2017;14:40–60.
32. Rani S, Salahuddin, Mazumder A, Kumar R, et al. Pyrazole/pyrazoline-bearing benzimidazoles: therapeutic exploration. Curr Org Chem. 2025.
33. Babbar R. Therapeutic potential of Schiff and Mannich bases of 2-substituted benzimidazoles. Int J Drug Del Technol. 2022.
34. Ouaket A, Moughaoui F, Laaraibi A, et al. DPPH scavenging of bis-benzimidazole derivatives. Med J Chem. 2019;8:103–107.
35. Gaba M, Mohan C. Drug development with imidazole & benzimidazole heterocycles. Med Chem Res. 2016;25:173–210.

.